

## Giant Effect of Uniaxial Pressure on Magnetic Domain Populations in Multiferroic Bismuth Ferrite

M. Ramazanoglu,<sup>1</sup> W. Ratcliff II,<sup>2</sup> H. T. Yi,<sup>1</sup> A. A. Sirenko,<sup>3</sup> S.-W. Cheong,<sup>1</sup> and V. Kiryukhin<sup>1</sup>

<sup>1</sup>*Department of Physics and Astronomy, Rutgers University, Piscataway, New Jersey 08854, USA*

<sup>2</sup>*NIST Center for Neutron Research, National Institute of Standards and Technology, Gaithersburg, Maryland 20899, USA*

<sup>3</sup>*Department of Physics, New Jersey Institute of Technology, Newark, New Jersey 07102, USA*

(Received 31 May 2011; published 3 August 2011)

Neutron diffraction is used to show that small ( $\sim 7$  MPa, or 70 bar) uniaxial pressure produces significant changes in the populations of magnetic domains in a single crystal of 2% Nd-doped bismuth ferrite. The magnetic easy plane of the domains converted by the pressure is rotated  $60^\circ$  relative to its original position. These results demonstrate extreme sensitivity of the magnetic properties of multiferroic bismuth ferrite to tiny (less than  $10^{-4}$ ) elastic strain, as well as weakness of the forces pinning the domain walls between the cycloidal magnetic domains in this material.

DOI: 10.1103/PhysRevLett.107.067203

PACS numbers: 75.85.+t, 75.25.-j, 75.60.-d, 75.80.+q

Materials possessing several “functional” properties—the multifunctional materials—attract significant attention because of their unusual physical characteristics and their potential for applications. An important class of these materials is multiferroics, which combine ferroelectricity (FE) and magnetic order [1]. These functional properties of multiferroics can be controlled by applied electric and magnetic fields, as well as by strain, giving rise to a number of potentially applicable cross-coupling effects.  $\text{BiFeO}_3$  (BFO) is, arguably, the most widely studied multiferroic because it exhibits both large electric polarization ( $\sim 10^2 \mu\text{C}/\text{cm}^2$ ), and magnetic order at room temperature [2]. FE and magnetism are strongly coupled in BFO, and both control of the electric polarization by an applied magnetic field and rotation of spins by an electric field have been demonstrated [2–5].

Elastic strain is also strongly coupled to the multiferroic properties of BFO. The effects of hydrostatic pressure, anisotropic tensile, and compressive strain in thin films, as well as effects of chemical pressure in BFO have been studied extensively [2,6–9]. It is well known that both the crystallographic and magnetic structures of BFO change at hydrostatic pressures exceeding 5 GPa and at strains exceeding  $10^{-2}$ . As discussed below, BFO has a cycloidal magnetic structure at ambient pressure. This structure exhibits neither a ferromagnetic moment nor a linear magnetoelectric effect [10–12]. Large strain in thin films has been reported to suppress the cycloid [2], leading to the apparent emergence of both of these highly desirable properties [11–13]. The associated potential enhancement of the magnetoelectric response in BFO emphasizes the importance of harnessing the effects of strain in this material.

In this work, we report that uniaxial strains smaller than those quoted above by as much as 3 orders of magnitude can significantly affect the magnetic properties of BFO. Specifically, we find that uniaxial pressure induces changes in the magnetic domain populations which are

accompanied by a  $60^\circ$  rotation of the plane of the magnetic cycloid. We note that a change in the sample dimensions similar to that achieved in our experiments occurs due to thermal expansion upon changing the temperature by just 10 K. Such an extreme sensitivity of magnetism to uniaxial strain should be useful for fine control of the magnetic domain structure, which is an important requirement for construction of prototype BFO-based multiferroic devices. It can also play an important role in the giant effects of an electric field on the magnetic dynamics and domain structure exhibited by BFO.

At room temperature, BFO exhibits an  $R3c$  rhombohedral perovskite structure. We describe it using the pseudocubic notation with  $a \sim 3.96 \text{ \AA}$  and  $\alpha \sim 89.4^\circ$ . The electric polarization is along the (111) direction. The magnetic order is of the antiferromagnetic  $G$  type, with a long-range ( $\lambda \sim 620\text{--}670 \text{ \AA}$ ) cycloidal modulation superimposed [14–16]. This modulation can propagate along three directions equivalent by symmetry, described by propagation vectors  $\tau_1 = \delta(1, -1, 0)$ ,  $\tau_2 = \delta(1, 0, -1)$ , and  $\tau_3 = \delta(0, -1, 1)$ , where  $\delta \sim 0.0042$  reciprocal lattice units (r.l.u.) For each of the three cycloids, the spins rotate in the plane defined by the (111) and  $\tau$  vectors, see Fig. 1(a).

Neutron diffraction experiments were carried out at room temperature on the BT-9 triple axis spectrometer at the NIST Center for Neutron Research. The neutron energy of 14.7 meV and collimations 40-40-S-40-open were used. Pyrolytic graphite filters were installed before and after the sample to suppress  $\lambda/2$  contamination of the neutron beam. The samples were placed in a spring-loaded uniaxial pressure cell made of aluminum, that attenuates the neutron beam only slightly. Pure ( $x = 0$ ) and Nd-doped  $\text{Bi}_{1-x}\text{Nd}_x\text{FeO}_3$  single crystals were grown using flux method as described in Ref. [5]. Nd content was measured using neutron activation analysis. The pressure was applied to the polished cubic faces of the sample, parallel to the (001) axis, see Fig. 1. BFO crystals crack easily, and most

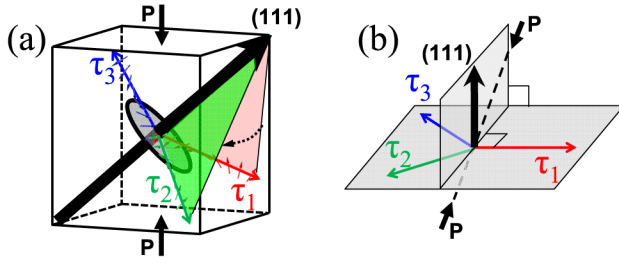


FIG. 1 (color online). (a) Magnetic cycloid wave vectors  $\tau_i$ , the (111) direction normal to these vectors, and the direction of the applied pressure  $P$  in the pseudocubic unit cell of  $\text{BiFeO}_3$ . The spins are confined in the 3 “easy” planes defined by the (111) and the  $\tau_i$  vectors. Two of these planes are shaded, and the dotted arrow shows the pressure-induced rotation of the spins from one of these planes to another. Panel (b) illustrates lifting of the magnetic domain degeneracy by pressure, as explained in the text.

samples do not survive even small pressures. Herein, we discuss an  $x = 0.022(2)$  Nd-doped BFO sample that sustained the pressure successfully. The entire 30 mg sample was one FE domain, as confirmed by studies of representative nuclear Bragg peaks. At such a small Nd doping, the material exhibits virtually the same structural and magnetic properties as the pure BFO [9]. We therefore believe that the obtained qualitative results also correctly represent the behavior of the pure system.

Magnetic domains  $\tau_i$  ( $i = 1, 2, 3$ ) produce magnetic Bragg peaks at  $Q_0 \pm \tau_i$ , where  $Q_0 = (0.5, 0.5, 0.5)$ . Figure 2 shows magnetic scattering near  $Q_0$  in the scattering plane containing the (111) and  $\tau_1$  vectors. This plane contains the “in-plane” domain  $\tau_1$  that produces a peak at the  $Q_0 \pm \tau_1$  positions. The “out-of-plane” domains  $\tau_2$  and  $\tau_3$ , while not in the scattering plane, produce the overlapping signal at the  $Q_0 \pm \tau_1/2$  positions due to the relaxed experimental resolution normal to the scattering plane, see Fig. 2(a). The scans through  $Q_0$  in the direction of  $\tau_1$  shown in Figs. 2(b)–2(d) were fitted with 2 equal Gaussian peaks at  $Q_0 \pm \tau_1$ , and 2 other equal peaks at  $Q_0 \pm \tau_1/2$ . The ratio of the integrated intensity of the first pair of peaks to that of the second gives the ratio of the in-plane to the out-of-plane magnetic domain populations. Such analysis for the virgin sample at zero pressure is shown in Fig. 2(b). It gives  $f_1 = 30\%$  for the initial population of the domain  $\tau_1$ . The analogous scan taken in the scattering plane based on (111) and  $\tau_3$  (not shown) gives  $f_2 = 10\%$  and  $f_3 = 60\%$  for the  $\tau_2$  and  $\tau_3$  initial domain populations, respectively, with an error bar of  $\sim 10\%$ . The value of  $\delta$  obtained from these scans is 0.0039 r.l.u., giving a slightly larger period of the cycloidal modulation  $\lambda = 720 \text{ \AA}$  than that of pure BFO at the same temperature [14–16]. Scans taken under applied uniaxial pressure are shown in Fig. 2(c). With increasing pressure ( $P$ ), the double-peak scans evolve into one broad peak at  $P \approx 7 \text{ MPa}$  (equal to 70 bar, or 70 atm). At higher pressures, this peak essentially did not change until the sample broke at  $P \sim 15 \text{ MPa}$ . The data at  $P = 7.2 \text{ MPa}$

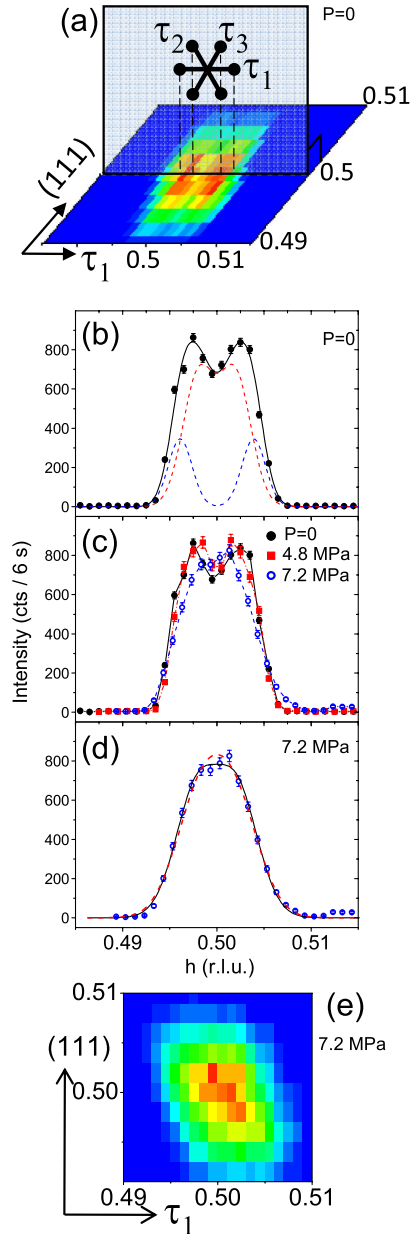


FIG. 2 (color online). Magnetic scattering in the vicinity of  $Q_0 = (0.5, 0.5, 0.5)$  in the plane defined by (111) and  $\tau_1$ . (a) The initial scattering pattern at  $P = 0$ . (b) The initial zero-pressure scan through  $Q_0$  along the  $\tau_1$  direction. The solid line is the fit described in the text, the dashed lines show the corresponding in- and out-of-plane domain contributions. (c) Scans taken at different uniaxial pressures. (d) The scan at  $P = 7.2 \text{ MPa}$  and the fits with zero (dashed line) and nonzero (solid line) in-plane domain contributions, as discussed in the text. (e) The scattering pattern at  $P = 7.2 \text{ MPa}$ . The tilted shape of the peak is due to instrumental resolution effects. In all panels, error bars (1 standard deviation) are from counting statistics.

are well described by assuming a total absence of the in-plane domain and the same  $\delta = 0.0039 \text{ r.l.u.}$ ; see the fit shown with dashed line in Fig. 2(d). Only a marginally better agreement with the data is obtained when the

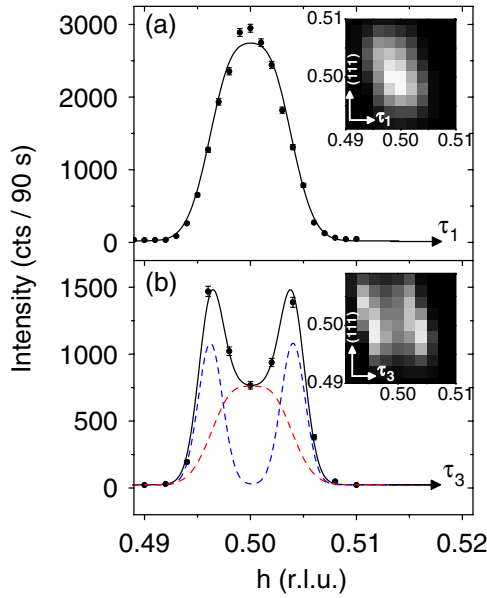


FIG. 3 (color online). Scans through the  $Q_0$  position along  $\tau_1$  (a), and along  $\tau_3$  (b) directions taken at  $P = 0$  after the pressure was applied and then removed. The insets show the overall scattering patterns in the corresponding scattering planes. Solid lines are fits described in the text. Dashed lines in (b) show the calculated in- and out-of-plane domain contributions to scattering. Error bars (1 standard deviation) are from counting statistics.

in-plane domain population is fitted; see the solid line in the same figure. The obtained population of domain  $\tau_1$  is then approximately 10%—still significantly smaller than that in the virgin sample at  $P = 0$ .

Two 5 mg fragments of the original sample were studied after the pressure was removed. The second fragment was kept at room temperature and studied 4 months after the original experiment was done. Both of the fragments exhibited the same properties. The magnetic scattering in the plane of (111) and  $\tau_1$  was found to be virtually identical to that measured at  $P > 7$  MPa; see the scans and meshes shown in Figs. 2(d), 2(e), and 3(a). The new zero-pressure data were collected in all the 3 scattering planes based on (111) and  $\tau_i$ ,  $i = 1, 2, 3$ . These data show that the magnetic cycloid has the same  $\delta = 0.0039$  r.l.u. as in the virgin sample. The fits shown in Figs. 3(a) and 3(b) show that the new domain populations are  $f_1 = 0$ ,  $f_2 = 50\%$ , and  $f_3 = 50\%$  (with the same  $\sim 10\%$  accuracy). Therefore, we conclude that application of  $\sim 7$  MPa uniaxial pressure in the (001) direction resulted in the conversion of the  $\tau_1$  domain, initially at one third population, into the other magnetic domains (primarily into  $\tau_2$ ). This change involves rotation of the plane of the magnetic cycloid by  $60^\circ$ , as shown in Fig. 1(a). It persists when the pressure is removed (for at least 4 months at constant temperature). A possible reason for such stability could be a tiny remanent strain favoring the pressure-induced state.

Uniaxial strain should result in direction-dependent changes in the magnetic couplings between the Fe spins,

making the free energies of domains  $\tau_i$  different. As shown in Fig. 1(b), application of pressure along (001) lifts the degeneracy of the  $\tau_i$  vectors, making  $\tau_1$  special, and leaving  $\tau_2$  and  $\tau_3$  degenerate. The crystal lattice along the  $\tau_2$  and  $\tau_3$  directions becomes compressed in comparison to the  $\tau_1$  direction. Assuming that the magnetic coupling increases with the lattice compression, this favors domains  $\tau_2$  and  $\tau_3$  energetically. This agrees with the observed selective suppression of the  $\tau_1$  domain.

The large effect of strain on the magnetic domain populations demonstrates weakness of the domain wall pinning forces. While large literature exists on the properties (including magnetic) of the FE walls in BFO [17], the nature of the purely magnetic walls between the  $\tau_i$  domains has not been studied in any detail. In related systems with parallel cycloids in the magnetic domains, a number of intriguing effects were predicted, including the existence of planar and linear (vortexlike) topological defects [18]. In BFO, vectors  $\tau_i$  are noncollinear, creating the potential for new nontrivial domain wall properties, such as topological defects. Theoretical studies of these domain walls are therefore highly desired. At this stage, we can only note that because of the large wavelength of the cycloid and noncollinear cycloid propagation vectors, domain walls in BFO are likely to be thick. Large domain wall thickness promotes averaging out of the pinning forces, in agreement with our data. These conclusions are, of course, qualitative, and the microscopic mechanism of the observed effects remains to be revealed. Real-space imaging of the magnetic domains is also of interest. Such imaging could be possible because of a theoretically predicted small local ferromagnetic moment normal to the cycloidal planes [11]. Further experimental and theoretical work is clearly needed to explain the properties of BFO discussed here.

The Young's modulus of BFO is  $\sim 100$  GPa [19]. Therefore, the strain achieved in our measurements is  $10^{-5}$ – $10^{-4}$ , that is 2–3 orders of magnitude smaller than the strain needed for any structural transition [6–9]. In fact, such small strains can easily be produced in clamped samples (or even in those glued to a sample holder) due to thermal expansion upon just a 10 K temperature change (the linear thermal expansion coefficient of BFO is  $\sim 1 \times 10^{-5}$  K $^{-1}$  at room temperature) [20]. We note that in strain-free setups, domain populations can, nevertheless, be stable in an extended temperature range [15]. Rotation of the magnetic cycloid plane due to temperature-induced strain can mimic magnetic anomalies. Our results could therefore be relevant for understanding of some of the numerous transitions of so far unestablished origin reported in BFO [2,19,21,22] which keep attracting significant attention of both theoreticians [23] and experimentalists [24]. Perhaps even more importantly, strain-induced rotation of the magnetic cycloid plane could play a role in the dramatic effects of an applied electric field ( $E$ ) on

magnetism reported in BFO. Examples include a  $\sim 30\%$  change of magnon frequencies [25] for  $E \sim 100$  kV/cm, and field-induced changes [26] of the domain populations for  $E \sim 10$  kV/cm. The former result was explained by direct coupling of the Néel order parameter to  $E$  via spin-orbit coupling, while in the latter work piezoelectric effects were considered. Because of piezoelectric striction, fields of these magnitudes produce anisotropic strain in the  $10^{-5}$ – $10^{-4}$  range, similar to the strain achieved in our studies ( $d_{33} \sim 10$ – $50$  pm/V in BFO) [27]. Thus, the field-induced strain might significantly affect magnetic domain populations in these experiments. Magnetic properties, such as magnon frequencies for a certain propagation direction, can be affected by piezoelectricity and magnetostriction, and should depend strongly on the orientation of the magnetic cycloid [28]. The field-induced strain can, therefore, be one of the mechanisms underlying the effects observed in an applied electric field. Our results show that a knowledge of magnetic domain populations is essential for understanding the effects of an electric field in BFO, and that these populations should be determined before definitive conclusions about the observed effects are made. Finally, we note that lattice strains comparable to those discussed above should be achievable in thin films with the appropriate substrate and thickness. These films could exhibit effects similar to those reported here. Dependence of their magnetic domain properties on temperature, electric, and magnetic fields, and other probes is, in our opinion, an intriguing subject for future work.

In summary, we report that magnetic domain populations in BFO can be changed by a uniaxial pressure as small as a few tens of atmospheres. The pressure-induced change involves rotation of the plane of the magnetic cycloid by  $60^\circ$ . These results show that the magnetic domains (and, consequently, the orientation of the magnetic easy plane) can easily be controlled by an external stress. They also emphasize importance of induced strain for BFO's magnetic properties in an applied electric field.

This work was supported by the NSF under Grant No. DMR-1004568 and No. DMR-0804109.

- [1] S-W. Cheong and M. Mostovoy, *Nature Mater.* **6**, 13 (2007).
- [2] For a review, see G. Catalan and J.F. Scott, *Adv. Mater.* **21**, 2463 (2009).
- [3] Y.F. Popov *et al.*, *JETP Lett.* **57**, 69 (1993).
- [4] T. Zhao *et al.*, *Nature Mater.* **5**, 823 (2006).
- [5] S. Lee *et al.*, *Appl. Phys. Lett.* **92**, 192906 (2008).
- [6] R. Haumont *et al.*, *Phys. Rev. B* **79**, 184110 (2009).
- [7] A.J. Hatt, N.A. Spaldin, and C. Ederer, *Phys. Rev. B* **81**, 054109 (2010).
- [8] D. Kan *et al.*, *Adv. Funct. Mater.* **20**, 1108 (2010).
- [9] I. Levin *et al.*, *Phys. Rev. B* **81**, 020103(R) (2010).
- [10] A.M. Kadomtseva *et al.*, *JETP Lett.* **79**, 571 (2004).
- [11] C. Ederer and N.A. Spaldin, *Phys. Rev. B* **71**, 060401 (2005).
- [12] D. Albrecht *et al.*, *Phys. Rev. B* **81**, 140401(R) (2010).
- [13] H. Béa *et al.*, *Appl. Phys. Lett.* **87**, 072508 (2005).
- [14] I. Sosnowska, T. Peterlin-Neumaier, and E. Steichele, *J. Phys. C* **15**, 4835 (1982).
- [15] M. Ramazanoglu *et al.*, *Phys. Rev. B* **83**, 174434 (2011).
- [16] J. Herrero-Albillos *et al.*, *J. Phys. Condens. Matter* **22**, 256001 (2010).
- [17] J. Seidel *et al.*, *Nature Mater.* **8**, 229 (2009); A. Lubk, S. Gemming, and N.A. Spaldin, *Phys. Rev. B* **80**, 104110 (2009).
- [18] A.N. Bogdanov *et al.*, *Phys. Rev. B* **66**, 214410 (2002); V.A. Lykah, *Ferroelectrics* **398**, 71 (2010).
- [19] S.A.T. Redfern *et al.*, *J. Phys. Condens. Matter* **20**, 452205 (2008).
- [20] A. Palewicz *et al.*, *Solid State Commun.* **140**, 359 (2006).
- [21] M.K. Singh, R.S. Katiyar, and J.F. Scott, *J. Phys. Condens. Matter* **20**, 252203 (2008); J.F. Scott, M.K. Singh, and R.S. Katiyar, *ibid.* **20**, 322203 (2008); J.F. Scott, M.K. Singh, and R.S. Katiyar, *ibid.* **20**, 425223 (2008); M.K. Singh *et al.*, *ibid.* **21**, 042202 (2009).
- [22] M. Cazayous *et al.*, *Phys. Rev. Lett.* **101**, 037601 (2008).
- [23] O. Diéguez *et al.*, *Phys. Rev. B* **83**, 094105 (2011).
- [24] X. Marti *et al.*, *Phys. Rev. Lett.* **106**, 236101 (2011).
- [25] P. Rovillain *et al.*, *Nature Mater.* **9**, 975 (2010).
- [26] S. Lee *et al.*, *Phys. Rev. B* **78**, 100101(R) (2008).
- [27] D. Lebeugle *et al.*, *Phys. Rev. B* **76**, 024116 (2007).
- [28] P. Rovillain *et al.*, *Phys. Rev. B* **79**, 180411(R) (2009).